Model and analysis of the interaction dynamics in cooperative manipulation tasks

Sebastian Erhart, *Student Member, IEEE,* Sandra Hirche, *Senior Member, IEEE*

Abstract—Efficient coordination of a multi-robot team is the key challenge in robotic application domains such as manufacturing, construction and service robotics. In cooperative manipulation tasks, the system dynamics result from the complex interaction of several manipulators handling a common object. A comprehensive model is indispensable for sophisticated model-based control design. An open problem is the modeling and the analysis of the overall system dynamics including the manipulators' interaction wrenches. Based on the apparent end-effector dynamics in task space, in this article we focus on the characterization of the interaction effects when manipulating a common object. We point out the central role of the imposed kinematic constraints for the emerging system dynamics, their significance for the manipulator coordination in terms of control design and the analysis of internal wrenches applied to the object. We derive fundamental properties of the cooperative manipulator system relevant to the manipulation task such as the apparent impedance w.r.t. external disturbances. An experimental study is conducted with two cooperating, anthropomorphic manipulators supporting the relevance of our findings.

Index Terms—Cooperative Manipulators, Interaction Dynamics, Internal Stress, Dynamics, Kinematics.

I. Introduction

COOPERATIVE manipulation tasks are characterized by the joint coordination of several robots handling a common object. A team of multiple manipulators is needed in tasks exceeding the capacity of a single manipulator in terms of payload or dexterity. Application domains include manufacturing, construction, agriculture and forestry, service robotics, search and rescue but also cooperative aerial manipulation. The benefits of using a team of robots for manipulating a common object come at the cost of an increased complexity for coordinating the manipulator ensemble when cooperatively implementing a force/motion control scheme. The effective behavior of the cooperative manipulator system is determined by the interaction of the local, generally nonlinear manipulator dynamics and the dynamics of the manipulated object. The interplay between the cooperative coordination strategy, the manipulator force/motion control schemes and the interaction forces needs to be thoroughly analyzed for a successful implementation of cooperative manipulation tasks. A concise interaction model is furthermore a prerequisite for deriving model-based control strategies. In this article we focus on the modeling of the interaction dynamics of cooperative manipulators but not on the control design itself.

Cooperative manipulator systems have been studied in the past. A pioneering work on the dynamics of a robotic multi-arm system under motion constraints is given in [1]. The *augmented*

object model describing the apparent dynamics of a cooperating manipulator system is presented in [2]. The authors of [3]–[6] present a model of the cooperative manipulator dynamics illustrating the interaction effects in joint space. More recently, the modeling of the redundant manipulator dynamics are interpreted in the context of constrained multi-body systems [7], [8]. These previous works build on the formulation of the interaction dynamics in joint space without addressing relevant interaction effects between the manipulators in task space. In [9] the interaction between cooperative manipulators is modeled in task space by means of port-Hamiltonian systems without addressing the underlying Dirac structure. For a more general treatment of Dirac structures, the interested reader is referred to [10] or [11] and references therein. The Dirac structure determines the interaction wrenches and is thus a central quantity for manipulation tasks. As will be detailed in the sequel, manipulation of a rigid object gives rise to kinematic constraints between the manipulators' end-effectors, leading to an *implicit* port-Hamiltonian system endowed with a Dirac structure and thus to a mixed set of differential and algebraic equations (DAEs) [12]. The Dirac structure induced from a constraint distribution may be represented in various ways [11] among which the Lagrange multiplier formulation is the most common. The Dirac structure and the underlying rigidity constraints between the end-effectors have not been explored for the modeling of cooperating manipulators in the robotics literature. Moreover, there exists currently no explicit closed-form solution for computing the manipulators' end-effector wrenches in task space when cooperatively manipulating an object. It is obvious that such an expression is the core instrument for an accurate and compact numerical simulation tool of multi-robot manipulation tasks and the analysis and design of model-based cooperative coordination strategies, since it allows to quantify the end-effector wrenches applied to the object and provides insight on how the interaction between manipulators and object actually takes place.

A very similar situation in view of modeling and control design is encountered in dexterous manipulation of objects with multi-fingered hands. Interestingly, common models for the dynamics in dexterous manipulation *do* actually incorporate the coupling between fingertips and object in terms of a kinematic (velocity) constraint [13]. The interaction wrenches between fingers and object have a straightforward interpretation as the Lagrange multiplier associated to the kinematic constraints [14]. However, inertia terms are neglected and quasi-static manipulation is assumed when computing explicit values for the resulting interaction wrenches. Recent works on cooperative aerial manipulation as e.g. [15] assume quasi-static manipulation, too. This assumption does not longer

S. Erhart and S. Hirche are with the Chair of Information-oriented control, Technische Universität München, Arcisstraße 21, D-80290 München, Germany e-mail: {erhart,hirche}@tum.de.

hold when either manipulating very heavy objects even with low accelerations (e.g. cooperative pick and place tasks with industrial manipulators) or in case of lightweight objects with high accelerations (e.g. obstacle avoidance maneuver in aerial manipulation). Note that the presented modeling in this article incorporating equality constraints is valid for inequality constraints, too, as long as the applied finger forces in grasping and the wire forces for aerial manipulators remain positive.

The *control design* for cooperative manipulation tasks is commonly performed in task space without explicitly addressing the coupling of the manipulator dynamics. Based on the concept of impedance control [16], a cooperative control scheme realizing an apparent object impedance is proposed by the authors of [17] and [18]. A decentralized implementation of the object impedance scheme is presented in [19]. However, no conclusion is drawn on the resulting object impedance. Recent publications on the control design for dexterous manipulation are either assuming quasi-static object manipulation [20] or specify the desired closed-loop behavior through *virtual* object dynamics [21] without explicit model of the interaction wrenches. In general the control design for implicit port-Hamiltonian systems is found to be non-trivial [22]. It is obvious that a closed-form representation of the cooperative dynamics is a necessary prerequisite for advanced model-based cooperative control design, leading to a physically consistent formulation of internal/external force control schemes as recently published in [23].

The contribution of this article is a compact, complete and physically consistent model of the interaction dynamics of a cooperative manipulator system in task space. We show that the kinematic constraints imposed on the manipulators by rigidly grasping a common object constitute the quintessential characteristics for the analysis of the interaction dynamics. Unlike previous works we intentionally reduce the discussion of the explicit joint space dynamics of the manipulators to a minimum. Instead, by considering only the manipulators' apparent end-effector dynamics we provide a new perspective on the relevant interaction effects in task space. Our results bridge the gap between previous modeling approaches in joint space and existing control methodologies in task space. Although we employ impedance control schemes for the individual manipulators, we are not addressing the control design but are focusing on the modeling of the interaction effects such as the explicit computation of the manipulators' interaction forces/torques and internal wrenches. To this end, we apply Gauss' principle of least constraint [24] to the apparent end effector dynamics, transforming the model of the interaction dynamics from the initial implicit (DAE) representation to a system of explicit ordinary differential equations (ODEs). As a direct consequence we obtain a compact and explicit closed-form solution for the manipulators' interaction wrenches for arbitrary dynamic manipulation tasks. Based on this new perspective on the cooperative manipulator system as a constrained multi-body system, we derive fundamental system properties relevant for the manipulation task, as e.g. the apparent object impedance when employing the distributed impedance control scheme and prove passivity of the cooperative dynamics relevant for the interaction with the environ-ment. Our results are validated in an experimental study.

The remainder of this article is organized as follows. Section II presents the dynamics of manipulators and object. Section III deals with the modeling of the interaction dynamics. In Section IV we present model properties relevant to the cooperative manipulation task. Section V contains the experimental validation before summarizing the article in Section VI.

II. SYSTEM DYNAMICS

In order to concentrate on the interaction effects of the manipulator team, we consider local impedance control schemes for each end-effector in task space and review briefly the dynamics of a rigid object in this section.

A. Manipulator dynamics

The desired impedance behavior for each of the N manipulators in task space can generally be achieved by applying local feedback linearization for inner-loop control and a suitable choice of control law for the outer-loop [25]. In order to shape the apparent inertia of the robotic end-effector in task space [26], we assume the presence of a force/torque sensor at the robot wrist. The compliant behavior of the i-th manipulator in task space is then given by

$$M_i \left[\ddot{x}_i - \ddot{x}_i^d \right] + D_i \left[\dot{x}_i - \dot{x}_i^d \right] + h_i^K(x_i, x_i^d) = h_i - h_i^d + \tilde{h}_i \quad (1)$$

wherein $x_i = (p_i^T, q_i^T)^T$ denotes the pose and $h_i = (f_i^T, t_i^T)^T$ the end-effector wrench of the i-th end-effector. The pose is split into translational and rotational coordinates with $p_i \in \mathbb{R}^3$ and the unit quaternion $q_i = \left(\eta_i, \epsilon_i^T \right)^T \in \mathrm{Spin}(3)$ wherein $\eta_i \in \mathbb{R}$ is the real part and $\epsilon_i \in \mathbb{R}^3$ is the imaginary part.. Thus each x_i can be mapped onto an element of the special Euclidean group $SE(3)$. The twist $\dot{x}_i = (\dot{p}_i^T, \omega_i^T)^T \in se(3)$ is a six-dimensional vector composed of the end-effector's translational and rotational velocity denoted by $\dot{p}_i \in \mathbb{R}^3$ and $\omega_i \in \mathbb{R}^3$.

Remark (Quaternion rates and angular velocity): Employing a slight abuse of notation, the twist $\dot{x}_i$ is *not* the pure time derivative of the pose x_i, in particular $\frac{d}{dt} q_i \neq \omega_i$. The proper conversion between quaternion rates and angular velocity is given by the following relation [27]

$$\begin{pmatrix} 0 \\ \omega_i \end{pmatrix} = 2Q^T(q_i)\dot{q}_i \quad (2)$$

and its inverse

$$\dot{q}_i = \frac{1}{2} Q(q_i) \begin{pmatrix} 0 \\ \omega_i \end{pmatrix} \quad (3)$$

with the matrix

$$Q(q_i) = \begin{bmatrix} \eta_i & -\epsilon_i^T \\ \epsilon_i & \eta_i I_3 + S(\epsilon_i) \end{bmatrix}. \quad (4)$$

I_3 is the 3×3 identity matrix. $S(\cdot)$ is the skew-symmetric matrix performing the cross-product operation, i.e. $a \times b = S(a) \cdot b = -S(b)a$.

The wrench h_i is split into the force and torque vectors $f_i, t_i \in \mathbb{R}^3$. Desired quantities are indicated by the superscript d. The disturbing wrench $\tilde{h}_i$ accounts for inaccuracies in the local feedback linearization. The term $\tilde{h}_i$ is in general time-varying and non-zero (but bounded) and vanishes in case of ideal feedback linearization. The impedance parameters $M_i, D_i, K_i \in \mathbb{R}^{6 \times 6}$ representing the apparent inertia, damping and stiffness are assumed to exhibit (block-)diagonal structure, i.e. $M_i = \mathrm{diag}(m_i I_3, J_i)$, $D_i = \mathrm{diag}(d_i I_3, \delta_i I_3)$ and $K_i = \mathrm{diag}(k_i I_3, \kappa_i I_3)$, decoupling the translational from the rotational behavior. The matrices are parameterized by the scalar values $m_i, d_i, k_i \in \mathbb{R}^+$ yielding isotropic translational behavior of the individual end-effector. $\mathbb{R}^+$ denotes the set of strictly positive real numbers. The rotational dynamics are determined by the positive definite inertia matrix $J_i \in \mathbb{R}^{3 \times 3}$ and the scalar parameters $\delta_i, \kappa_i \in \mathbb{R}^+$. The geometrically consistent stiffness h_i^K [28] is given by

$$h_i^K(x_i, x_i^d) = \begin{pmatrix} f_i^K \\ t_i^K \end{pmatrix} = \begin{pmatrix} [k_i I_3] \, \Delta p_i \\ [\kappa_i' I_3] \, \Delta \epsilon_i \end{pmatrix} \qquad (5)$$

wherein the difference of actual and desired pose is defined as $\Delta p_i = p_i - p_i^d$ and $\Delta q_i = q_i * (q_i^d)^{-1}$ with $\kappa_i' = 2\Delta\eta_i \kappa_i$ and the operator $*$ denoting the quaternion product. For notational convenience the quaternion expressing the relative orientation is further split into $\Delta q_i = \left(\Delta\eta_i, \Delta\epsilon_i^T\right)^T$.

All terms in the end-effector dynamics (1) related to the kinematic motion control are subsequently referred to as

$$h_i^x = M_i \ddot{x}_i^d - D_i[\dot{x}_i - \dot{x}_i^d] - h_i^K(x_i, x_i^d). \qquad (6)$$

B. Object dynamics

The equations of motion of a rigid object are derived by applying Lagrangian mechanics. The object's kinetic and potential energy are

$$T_o = \frac{1}{2}\dot{x}_o^T M_o \dot{x}_o \quad \text{and} \quad U_o = m_o \, g^T p_o \qquad (7)$$

with $M_o = \mathrm{diag}(m_o I_3, J_o)$ and $m_o \in \mathbb{R}$ and $J_o \in \mathbb{R}^{3 \times 3}$ are the object's mass and inertia respectively and $g \in \mathbb{R}^3$ is the gravity vector. For convenience of notation we omit the explicit indication of dependencies such as $M_o(x_o)$ when unambiguous. Employing (7) for deriving the Lagrange equations yields the object dynamics w.r.t. to its center of mass

$$M_o \ddot{x}_o + C_o \dot{x}_o + h_g = h_o + \tilde{h}_o \qquad (8)$$

wherein h_o is the effective wrench acting on the object due to the interaction with the manipulators, $\tilde{h}_o$ is a disturbance from an external force and h_g and C_o incorporate the gravity force and the Coriolis term, i.e.

$$h_g = \begin{pmatrix} -m_o \, g \\ 0_{3 \times 1} \end{pmatrix} , \quad C_o = \begin{bmatrix} 0_3 & 0_3 \\ 0_3 & \omega_o \times J_o \end{bmatrix}. \qquad (9)$$

III. INTERACTION DYNAMICS

We are now interested in the dynamic behavior of the cooperative system when the manipulators are rigidly grasping the object. The manipulation of a common object gives rise to kinematic constraints restricting mutually the manipulators' motion which will be discussed in the following subsection. The emerging system dynamics subject to the kinematic constraints gives rise to the interaction wrenches as discussed in the second subsection. The extension of our modeling approach to alternative manipulator control schemes is presented in the last subsection.

A. Kinematic constraints

The manipulated object is assumed to be rigid and the end-effectors are assumed to be rigidly connected to the object. For the subsequent mathematical description of the constraints a coordinate system is attached to each rigid body. This situation is depicted in Fig. 1.
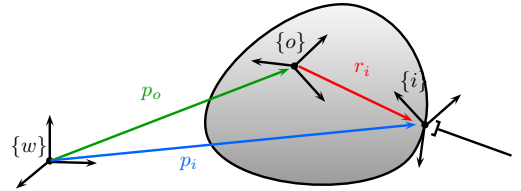

Fig. 1. Illustration of the coordinate systems

The coordinate frames are denoted by curly brackets. Besides the body-fixed object frame $\{o\}$ each manipulator has its individual, local end-effector frame $\{i\}$. If not stated otherwise (through a leading upper index) vectors are expressed in the (inertial) world frame $\{w\}$.

1) Translational constraint: The rigidity condition constrains the relative displacement of two bodies, i.e. $^o r_i = \text{const}$. This means that the relative position of the manipulator with respect to the body-fixed coordinate system $\{o\}$ remains constant. Using this fact one may express the position of the i-th end effector as $p_i = p_o + {}^w R_o(q_o) \, {}^o r_i$ with the 3×3 rotation matrix $^w R_o$ transforming a vector from frame $\{o\}$ to frame $\{w\}$. Differentiation of p_i and using $^o r_i = \text{const}$. yields

$$\dot{p}_i = \dot{p}_o + \omega_o \times r_i. \qquad (10)$$

Differentiating (10) again leads to

$$\ddot{p}_i = \ddot{p}_o + \dot{\omega}_o \times r_i + \omega_o \times (\omega_o \times r_i). \qquad (11)$$

This latter condition constrains mutually the admissible accelerations of the object $\ddot{p}_o$, $\dot{\omega}_o$, the end-effector $\ddot{p}_i$ and the object's angular velocity ω_o.

2) Rotational constraint: Furthermore the relative orientation between object and manipulators $^o \delta q_i = q_o^{-1} * q_i$ is constrained to remain constant, i.e. $^o \delta q_i = \text{const}$. Differentiation of $^o \delta q_i$ w.r.t. time reveals that the angular velocity of the two bodies $\{o\}$ and $\{i\}$ needs to be equal [23, Lemma 1], such that $\omega_o = \omega_i$. Thus one has after differentiating again

$$\dot{\omega}_o = \dot{\omega}_i \tag{12}$$

imposing a constraint on the admissible angular acceleration of the object and the end-effector.

3) Constraint matrix: In order to analyze the system dynamics under constraints, it is convenient to introduce the stacked state vector $x = \left(x_o^T, x_1^T, \ldots, x_N^T\right)^T$ being an element of the (N+1)-fold Cartesian product of $SE(3)$ and containing the stacked pose information of object and end-effectors. The corresponding acceleration vector reads thus $\ddot{x} = \left(\ddot{p}_o^T, \dot{\omega}_o^T, \ddot{p}_1^T, \dot{\omega}_1^T, \ldots \ddot{p}_N^T, \dot{\omega}_N^T\right)^T \in \mathbb{R}^{6\cdot(N+1)}$. The acceleration constraints (11) and (12) may be rewritten compactly as

$$A \cdot \ddot{x} = b \tag{13}$$

with $A \in \mathbb{R}^{6\cdot N \times 6\cdot(N+1)}$ and $b \in \mathbb{R}^{6\cdot N}$ given by

$$A = \begin{bmatrix} -I_3 & S(r_1) & I_3 & 0_3 & & 0_3 & 0_3 \\ 0_3 & -I_3 & 0_3 & I_3 & & 0_3 & 0_3 \\ \vdots & \vdots & & & \ddots & & \\ -I_3 & S(r_N) & 0_3 & 0_3 & & I_3 & 0_3 \\ 0_3 & -I_3 & 0_3 & 0_3 & & 0_3 & I_3 \end{bmatrix} \tag{14}$$

and $b = [(S(\omega_o)^2 r_1)^T, \ldots, (S(\omega_o)^2 r_N)^T]^T$. 0_3 is the 3×3 zero matrix.

B. Constrained dynamics

Recall that the dynamics of the manipulators is imposed independently from each other through an impedance control law. By rearranging terms in (1) one has

$$M_i \ddot{x}_i = h_i^\Sigma + h_i \tag{15}$$

wherein $h_i^\Sigma := h_i^x - h_i^d + \tilde{h}_i$ is a wrench depending on the individual end effector motion control scheme as in (6), the load distribution h_i^d and an external disturbance $\tilde{h}_i$. The object dynamics (8) can be cast into similar form yielding

$$M_o \ddot{x}_o = h_o^\Sigma + h_o \tag{16}$$

with $h_o^\Sigma := \tilde{h}_o - C_o \dot{x}_o$. Combining the dynamic equations of the end effectors (15) and the object (16) leads to

$$\begin{bmatrix} M_o & & & \\ & M_1 & & \\ & & \ddots & \\ & & & M_N \end{bmatrix} \cdot \ddot{x} = \begin{pmatrix} h_o^\Sigma \\ h_1^\Sigma \\ \vdots \\ h_N^\Sigma \end{pmatrix} + \begin{pmatrix} h_o \\ h_1 \\ \vdots \\ h_N \end{pmatrix}. \tag{17}$$

The dynamics (17) can be interpreted as follows: the vector $h^\Sigma := \left(h_o^\Sigma, h_1^\Sigma, \ldots, h_N^\Sigma\right)^T$ contains the wrenches resulting from the *local* system dynamics. The vector $h := \left(h_o, h_1, \ldots, h_N\right)^T$ in turn results from the *global* interaction of all manipulators through the object. The vector h thus adopts suitable values to render the accelerations $\ddot{x}$ on the left-hand side of (17) compatible to the constraint (13) at any time instant and for any given h^Σ. The computation of the constraining wrench is a problem arising in the domain

of constrained multi-body systems. In fact an explicit solution for h is presented in [29] given by

$$h = P(b - AM^{-1}h^\Sigma) \tag{18}$$

with $P = M^{\frac{1}{2}}(AM^{-\frac{1}{2}})^\dagger$ and $M = \text{diag}(M_o, M_1, \ldots, M_N)$.

Discussion: The cooperative manipulator dynamics (17) in combination with the Dirac structure represented through an explicit expression for the interaction wrenches h in (18) constitutes for the first time a complete and physically consistent interaction model of the rigidly coupled manipulator system. Note that the vector h in (17) contains the actual end-effector wrenches h_1 to h_N as measurable by each manipulator by means of a wrist mounted force/torque sensor. The contribution of our modeling approach is that we provide a closed-form expression for *computing* the interaction wrenches instead of merely *measuring* them via force/torque sensors at the real end-effector. This is clearly a prerequisite for the consistent design of model-based force/torque controllers.

Remark: In previous modeling approaches for multi-robot manipulation [1]–[6], [30] and dexterous manipulation [13], [14] only implicit expressions for the constraining forces/torques based on the Lagrange multiplier formulation in terms of $h = \lambda \frac{\partial A}{\partial x}$ are presented. Equation (18) presents an explicit closed-form solution for computing the interaction wrenches and is an essential ingredient for the analysis of the dynamics and the control synthesis in manipulation tasks.

The derivation of this result is based on Gauss' principle of least constraint, which states that the acceleration of a constrained system is altered with respect to the acceleration of an equivalent unconstrained system such that the acceleration difference is minimal in the least-squares sense. The equivalent optimization problem is given by

$$\min_{\ddot{x}} \quad (\ddot{x} - \ddot{x}^\Sigma)^T M (\ddot{x} - \ddot{x}^\Sigma) \tag{19}$$
$$\text{subject to} \quad A\ddot{x} = b$$

with $\ddot{x}^\Sigma = M^{-1}h^\Sigma$ denoting the acceleration of the unconstrained system. The interpretation of the system dynamics (17) as the solution of a constrained optimization problem (19) admits interesting insights. Arbitrary trajectories in terms of x_i^d may be specified *a priori* for each manipulator. The desired trajectories in combination with the desired end-effector wrenches h_i^d determine unambiguously the virtual wrench vector h^Σ as a function of the manipulator control laws. In case that initially assigned trajectories are incompatible to the kinematically constrained system, the emerging end-effector wrenches h render the system trajectory compatible to the imposed constraints by means of (18).

The resulting block scheme of the constrained dynamics system is illustrated in Fig. 2.

Recall that the stacked wrench vector h^Σ is a function of the object and the individual end effector dynamics, incorporating the control gains and force/motion setpoints (cf. (15) and (16). The lower branch in Fig. 2 represents the projection of the cooperative dynamics on the kinematic constraints as given by (13). With respect to previous works, the output of the
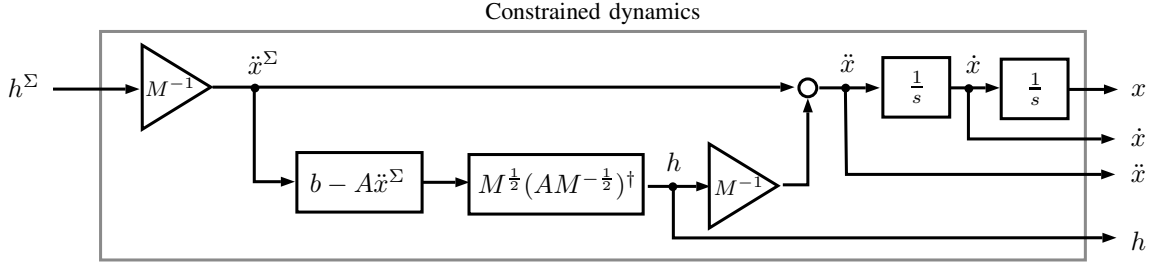
Constrained dynamics

Fig. 2. Block scheme representation of the constrained manipulator and object dynamics

presented model contains the resulting interaction wrenches h, computed by means of the closed-form expression (18).

C. Application to alternative manipulator control schemes

The impedance control law (1) presents a particular force control scheme for which a representation in the form of (17) is readily derived. Finding similar representations for alternative force control schemes (e.g. PI force controller [31]) is straightforward whenever the end-effector wrench h_i appears affine in the manipulator control law. But even pure motion control schemes which do not explicitly incorporate h_i can be interpreted by means of (17) by considering h_i as a disturbing end-effector wrench. Exemplarily a resolved acceleration control law combined with a PD tracking controller and feed forward acceleration term [25] is written as

$$h_i^\Pi = \Lambda_i[\ddot{x}_i^d - K_{D,i}(\dot{x}_i - \dot{x}_i^d) - K_{P,i}\,\Delta x_i] \qquad (20)$$

with the apparent inertia of the i-th end-effector Λ_i, the difference of actual and desired pose $\Delta x_i = [\Delta p_i^T, \Delta \epsilon_i^T]^T$ as in (5) and the proportional and derivative control gains $K_{P,i}$ and $K_{D,i}$. The local dynamics reads thus as

$$\Lambda_i \ddot{x}_i = h_i^\Pi + h_i, \qquad (21)$$

yielding a structurally similar expression as found for the impedance control law in (15). Note that Λ_i is the apparent *physical* inertia depending on the manipulator's specific inertial properties, whereas M_i in (1) is a *virtual* and tunable parameter by means of the impedance control law.

IV. COOPERATIVE MANIPULATION TASK

Based on the modeling of the cooperating manipulators in the previous section, we derive in the sequel some fundamental results relevant to the manipulation task.

A. Manipulator coordination

The manipulator coordination in cooperative manipulation tasks is commonly composed of a kinematic and a dynamic coordination strategy [32]. While the dynamic coordination determines the desired end-effector wrenches (setpoints for the force controller), the kinematic coordination is concerned with the computation of desired trajectories (setpoints for the motion controller) for the individual robotic end-effectors. Note that the wrench h_i in (1) denotes actually a quantity acting on the i-th end-effector. When interacting with the

object, due to Newton's third law, there will always be a wrench with opposite sign acting on the object, which will be denoted $\bar{h}_i$ in the sequel, such that

$$\bar{h}_i = -h_i \quad \text{and} \quad \bar{h}_i^d = -h_i^d. \qquad (22)$$

With above definition, the resulting object wrench h_o is computed according to

$$h_o = G\bar{h} \qquad (23)$$

with $\bar{h} = [\bar{h}_1, \ldots, \bar{h}_N]^T$. The grasp matrix G [33] incorporates explicitly the kinematic parameters defined via the constraints $r = [r_1^T, \ldots, r_N^T]^T$ as

$$G = \begin{bmatrix} I_3 & 0_3 & \cdots & I_3 & 0_3 \\ S(r_1) & I_3 & \cdots & S(r_N) & I_3 \end{bmatrix}. \qquad (24)$$

1) Dynamic coordination: Recently we proposed a more general approach to the problem of load distribution based on a novel, physically consistent definition [23].

Definition 1. *Internal wrenches are end-effector wrenches for which the total virtual work is zero for any virtual displacement of the end-effectors satisfying the kinematic constraints.*

All non-squeezing load distributions can be computed by means of a generalized inverse G_M^+ of the grasp matrix G in (23) as

$$G_M^+ = \begin{bmatrix} m_1^*[m_o^*]^{-1}I_3 & m_1^*[J_o^*]^{-1}S(r_1)^T \\ 0_3 & J_1^*[J_o^*]^{-1} \\ \vdots & \vdots \\ m_N^*[m_o^*]^{-1}I_3 & m_N^*[J_o^*]^{-1}S(r_N)^T \\ 0_3 & J_N^*[J_o^*]^{-1} \end{bmatrix} \qquad (25)$$

and positive definite weighting coefficients $m_i^* \in \mathbb{R}$ and $J_i^* \in \mathbb{R}^{3 \times 3}$ satisfying $m_o^* = \sum_i^N m_i^*$, $J_o^* = \sum_i^N J_i^* + \sum_i^N S(r_i)m_i^*S(r_i)^T$ and $\sum_i^N r_i m_i^* = 0_{3 \times 1}$, see [23] for more details.

Thus the desired end-effector wrenches implementing a desired object wrench h_o^d are given by

$$\bar{h}^d = G_M^+ h_o^d. \qquad (26)$$

2) Kinematic coordination: With the desired motion of the object $\dot{x}_o^d$ in hand, the desired motion of the end-effectors $\dot{x}_i^d$ is unambiguously determined by the following relation

$$\dot{x}^d = G^T \dot{x}_o^d, \tag{27}$$

with $\dot{x}^d = [(\dot{x}_1^d)^T, \ldots, (\dot{x}_N^d)^T]^T$ which is essentially a reformulation of the kinematic constraints presented in (11) and (12) at velocity level.

Remark: Based on $\dot{x}_i^d$, each manipulator is able to compute $\ddot{x}_i^d$ and x_i^d in its local end-effector frame by proper derivation/integration of the desired velocity. Equivalently, the desired trajectory x_i^d can locally be computed by double integration of $\ddot{x}_i^d$.

Employing above coordination strategies achieves force/motion tracking as presented in the following theorem.

Theorem 1. *Consider the object dynamics* (8) *and* (9) *without disturbance* $\tilde{h}_o = 0_{6\times 1}$ *and ideal feedback linearization* $\tilde{h}_i = 0_{6\times 1}$ *in* (1). *Further assume the object's inertia* M_o *and the grasp matrix* G *to be known. Then the combined dynamic and kinematic coordination strategies in* (26) *and* (27) *achieve tracking, i.e.*

$$h_o(t) \equiv h_o^d(t) \quad and \quad \dot{x}_o(t) \equiv \dot{x}_o^d(t) \tag{28}$$

for the cooperative manipulation task without applying internal wrenches according to Definition 1.

Proof. Ideal kinematic coordination of the manipulators according to (27) means that $\forall i : x_i(t) = x_i^d(t)$ which implies $\dot{x}_i = \dot{x}_i^d$ and $\ddot{x}_i = \ddot{x}_i^d$ in compliance with the kinematic constraints by construction. Using this fact in (1) (or in any other force/motion control scheme) one has immediately $h_i = h_i^d$ and $\bar{h}_i = \bar{h}_i^d$ respectively. Combining (23) and (26) leads to an explicit expression for the object wrench h_o in (8) as

$$h_o = GG_M^+ h_o^d. \tag{29}$$

By definition GG_M^+ is the identity matrix. Substituting this result in the object dynamics (8) and choosing $h_o^d = M_o \ddot{x}_o^d + C_o(x_o^d, \dot{x}_o^d)\dot{x}_o^d$ yields $\ddot{x}_o(t) = \ddot{x}_o^d(t)$ and thus $x_o(t) = x_o^d(t)$ for $x_o^d(0) = x_o(0)$ and $\dot{x}_o^d(0) = \dot{x}_o(0)$. No internal wrenches are applied to the object since the desired motion of the manipulators is by construction compatible to the kinematic constraints. Mathematically, this can be verified by employing $\ddot{x}'^x = \ddot{x}^d$ in (53) from which follows $h'_{\text{int}} = 0_{6\times 1}$. □

This result gives insight to the fundamental characteristics of a cooperative manipulation task. In general it is not sufficient to choose a suitable load distribution strategy for the manipulator ensemble but the effective end-effector motions need to be kinematically compatible to the imposed constraints, too. The control strategy of Theorem 1 achieves tracking and is essentially an inverse dynamics controller for the interaction dynamics model. The dynamic and kinematic coordination strategies (26) and (27) provide a dynamically consistent redundancy resolution. To the best of the authors' knowledge it is the first result on force/motion tracking for cooperating manipulators in task space which is based on a complete physical plant model of the manipulators.

B. Object impedance

In this subsection we present the resulting object dynamics with respect to a disturbing wrench. It turns out that the object behavior can again be characterized by an equivalent impedance in the form of (1) if the manipulators compensate the object's inertial effects.

Theorem 2. *Consider the impedance controlled end-effector dynamics* (1) *with ideal feedback linearization, i.e.* $\tilde{h}_i = 0_{6\times 1}$, *and assume the manipulator ensemble to compensate the gravity force of the object, i.e.* $h_o^d = h_g$ *in* (26). *Then the apparent dynamics of the cooperative manipulator system with respect to a disturbance* $\tilde{h}_o$ *in* (8) *is given by*

$$\mathcal{M}\ddot{x}_o + \mathcal{D}\dot{x}_o + h_o^K(x_o, x_o^d) + \mathcal{C}_o\dot{x}_o = \tilde{h}_o. \tag{30}$$

The apparent inertia $\mathcal{M}$, *damping* $\mathcal{D}$ *and stiffness* $\mathcal{K}$ *are*

$$\mathcal{M} = \begin{bmatrix} (m_o + \sum_i m_i)I_3 & \sum_i m_i S^T(r_i) \\ \sum_i S(r_i)m_i & \mathcal{J} \end{bmatrix} \tag{31}$$

with $\mathcal{J} := J_o + \sum_i J_i + \sum_i S(r_i)[m_i I_3]S^T(r_i)$,

$$\mathcal{D} = \begin{bmatrix} (\sum_i d_i)I_3 & \sum_i d_i S^T(r_i) \\ \sum_i S(r_i)d_i & \sum_i \delta_i + \sum_i S(r_i)[d_i I_3]S^T(r_i) \end{bmatrix} \tag{32}$$

and

$$h_o^K(x_o, x_o^d) = \sum_{i=1}^{N} \{ \begin{bmatrix} k_i I_3 & 0_3 \\ \Xi_i & \kappa_i' I_3 \end{bmatrix} \begin{pmatrix} \Delta p_o \\ \Delta \epsilon_o \end{pmatrix} \} \tag{33}$$

with the coupling terms $\Xi_i \in \mathbb{R}^{3\times 3}$ *defined by* $\Xi_i := S^T(r_i)k_i$. *For an infinitesimal twist displacement of the object* δx_o *about* x_o^d *in* (33) *one has* $h_o^K = \mathcal{K}\,\delta x_o$ *with*

$$\mathcal{K} = \sum_{i=1}^{N} \begin{bmatrix} k_i I_3 & 0 \\ \Xi_i & S^T(r_i)[k_i I_3]S(r_i) + \kappa_i I_3 \end{bmatrix}. \tag{34}$$

One particular factorization of the Coriolis-centrifugal matrix $\mathcal{C}_o$ *for the cooperative dynamics can be computed via*

$$\mathcal{C}_o\dot{x}_o = \dot{\mathcal{M}} - \frac{1}{2}\frac{\partial}{\partial x_o}\left(\dot{x}_o^T \mathcal{M}\dot{x}_o\right). \tag{35}$$

Proof. The apparent inertia of the object $\mathcal{M}$ is computed by considering the kinetic energy of the overall system being equivalent to the sum of the kinetic energy of the subsystems

$$T = T_o(\dot{x}_o) + \sum_{i=1}^{N} T_i(\dot{x}_i). \tag{36}$$

By employing the constraint (10) in (36) one has $T = \dot{x}_o^T \mathcal{M}\dot{x}_o$ yielding the expression for $\mathcal{M}$ in (31). Similar to the kinetic energy, the potential energy of the augmented system can be used to conclude on the apparent stiffness of the object $\mathcal{K}$. The potential energy of the overall system is the sum of the potential energy of the subsystems, i.e.

$$U = U_o(x_o) + \sum_{i=1}^{N} U_i(x_i). \tag{37}$$

The potential energy U_i depends implicitly on the desired pose of the i-th end-effector x_i^d since it is equivalent to the elastic energy stored in a tensioned spring between the points x_i and x_i^d with stiffness k_i/κ_i. The desired end-effector pose is chosen to coincide with the initial end-effector pose resulting in zero preload of all springs. By considering an arbitrary object equilibrium pose $\bar{x}_o = (\bar{p}_o^T, \bar{q}_o^T)^T$ the desired end-effector pose can be derived from the kinematic constraints

$$x_i^d = \begin{pmatrix} p_i^d \\ q_i^d \end{pmatrix} = \begin{pmatrix} \bar{p}_o +^w R_o(\bar{q}_o)^o r_i \\ \bar{q}_o * \delta q_i \end{pmatrix}. \tag{38}$$

It is worth noticing that the relative rotation of the object w.r.t. its equilibrium $\Delta q_o = q_o * (\bar{q}_o)^{-1}$ is equivalent to the relative rotation of the attached end-effectors w.r.t. their equilibrium pose, i.e. $\Delta q_i = \Delta q_o$. Thus the potential energy of the individual end-effector U_i in (46) can conveniently be written as a function of the object coordinates x_o according to

$$U_i(x_o) = \frac{1}{2}\Delta p_i^T[k_i I_3]\Delta p_i + 2\Delta\epsilon_o^T[\kappa_i I_3]\Delta\epsilon_o. \tag{39}$$

Taking the partial derivative of the potential energy U in (37) w.r.t. the object coordinates x_o yields $\frac{\partial U}{\partial x_o} = h_g + h_o^K(x_o)$ with the gravitational force h_g presented in (9) and $h_o^K(x_o)$ as given in (31). With the expressions for the kinetic and potential energy in (36) and (37) one readily derives the system's equation of motion by applying Lagrangian mechanics

$$\mathcal{M}\ddot{x}_o + \mathcal{C}_o\dot{x}_o + h_o^K(x_o) + h_g = h^* \tag{40}$$

wherein h^* is a generalized, non-conservative wrench acting on the object and $\mathcal{C}_o$ is the Coriolis-centrifugal matrix [34] associated to $\mathcal{M}$. For isotropic inertial parameters m_i and J_i the corresponding elements of $\mathcal{M}$ do *not* depend on the generalized coordinate x_o and the associated Christoffel symbols are thus zero. In this particular case one has $\mathcal{C}_o = C_o$ as in (9). The term h^* in (40) turns out to be of the form

$$h^* = -\mathcal{D}\dot{x}_o + h_o + \tilde{h}_o \tag{41}$$

with $\mathcal{D}$ given in (32). The expression for h^* can be derived by substituting (23) in the object dynamics (8) and replacing h_i by the impedance control law in (1). This yields

$$\mathcal{M}\ddot{x}_o + \mathcal{C}_o\dot{x}_o + \mathcal{D}\dot{x}_o + h_o^K(x_o) + h_g = h_o^d + \tilde{h}_o. \tag{42}$$

from which (30) follows immediately by letting $h_o^d = h_g$. □

This result has a straightforward interpretation in terms of a mechanical equivalent. The effective object inertia M_o is augmented by attaching rigidly the individual manipulator inertias M_i to the respective grasp points x_i. Additionally, for each manipulator a spring-damper element is attached at each grasp point with the remote suspension point located at the manipulators' desired pose x_i^d. The apparent damping and stiffness of the object results from a parallel connection of the individual spring-damper elements. Furthermore, the analytic expressions for $\mathcal{M}, \mathcal{D}$ and $\mathcal{K}$ in Theorem 2 constitute the

fundamental equations for the impedance synthesis in multi-robot cooperative manipulation tasks. Their significance is illustrated by the following example.

Example: Consider two manipulators with $k_1 = k_2 = 100\frac{\text{N}}{\text{m}}$, $\kappa_1 = \kappa_2 = 100\frac{\text{Nm}}{\text{rad}}$ and $^o r_{1/2} = \pm(1,0,0)^T$m. According to (34), the apparent translational stiffness of the object is isotropic and simply the parallel connection of k_1 and k_2 yielding $200\frac{\text{N}}{\text{m}}$. The rotational stiffness is the parallel connection of κ_1 and κ_2 plus the contribution from the translational stiffness yielding $(200, 400, 400)^T\frac{\text{Nm}}{\text{rad}}$ for infinitesimal rotations about the object axes. Even in case of a symmetric manipulator setup, the apparent stiffness of the object is non-isotropic. However, due to the symmetry the coupling term $\sum_i \Xi_i$ between translational and rotational motion is zero. The preceding observation for a symmetric setup of the manipulator system can further be generalized.

Corollary 1. *Let the values of m_i, d_i and k_i in (31), (32) and (33) respectively be homogeneous*

$$\forall i \neq j: \ m_i = m_j, \ d_i = d_j, \ k_i = k_j \tag{43}$$

and the grasp geometrically symmetric, that is $\sum_i r_i = 0_{3\times1}$. Then the translational and rotational object motion of the co-operative system (30) subject to a disturbance $\tilde{h}_o$ is decoupled, i.e. the matrices $\mathcal{M}$, $\mathcal{D}$ and $\mathcal{K}$ are block-diagonal.

Proof. It is straightforward to verify that the matrices $\mathcal{M}$, $\mathcal{D}$ and $\mathcal{K}$ are block-diagonal with zero off-diagonal matrices 0_3 by considering (31), (32) and (34) while employing (43) and exploiting the linearity of the skew-symmetric operator $S(\cdot)$ for $\sum_i r_i = 0_{3\times1}$. □

In the symmetric setup under consideration both the *center of stiffness* and the *center of compliance* [35] coincide with the origin of the object frame $\{o\}$, yielding perfect decoupling of translational and rotational behavior. Consider yet another practically motivated example.

Example: Assume that the apparent impedance of the cooperative manipulator system is to be tuned to exhibit critical damping. By considering the entries of $\mathcal{M}$, $\mathcal{D}$ and $\mathcal{K}$ in Theorem 2 it is obvious that the rotational impedance parameters involve the translational impedance parameters *and* the grasp kinematics in terms of r_i. Thus the impedance synthesis needs to incorporate the actual grasp geometry. An independent design of rotational and translational impedance leads in general not to the desired target impedance.

C. Stability of the interaction dynamics

We analyze subsequently the stability of the cooperative manipulator system. First we show strict output passivity of the interaction dynamics. A system is said to be output strictly passive [36, p. 236] if there exists a positive semidefinite storage function V and a positive definite function $y^T\rho(y)$ such that

$$u^T y \geq \dot{V} + y^T \rho(y) \tag{44}$$

for $y \neq 0$. The kinetic and potential energy of the object defined in (7) and the equivalent energy of the i-th manipulator

$$T_i = \frac{1}{2}\dot{x}_i^T M_i \dot{x}_i \tag{45}$$

$$U_i = \frac{1}{2}\Delta p_i^T[k_i I]\Delta p_i + 2\Delta\epsilon_i^T[\kappa_i I]\Delta\epsilon_i \tag{46}$$

are used in the storage function for the cooperative system

$$V = T_o + U_o + \sum_i \{T_i + U_i\}. \tag{47}$$

We are ready to state an intermediate result.

Lemma 1. *Assume that the manipulators compensate the gravity force of the object by choosing $h_o^d = h_g$ in (26) and (9) respectively. Then the system of object and manipulators (30) is strictly output passive with respect to the input $u = \tilde{h}_o$ and the output $y = \dot{x}_o$ with the storage function V in (47).*

Proof. The computation of the time derivative of (47) yields

$$\dot{V} = \dot{x}_o^T \mathcal{M}\ddot{x}_o + \frac{1}{2}\dot{x}_o^T \dot{\mathcal{M}}\dot{x}_o + \sum_{i=1}^N \{\Delta \dot{p}_i^T f_i^K + \Delta\omega_i^T t_i^K\}. \tag{48}$$

By substituting (42) in (48), letting $h_o^d = h_g$ and using the fact that $\dot{x}_o^T[\dot{\mathcal{M}} - 2\mathcal{C}_o]\dot{x}_o = 0$ (cf. [37]) leads to

$$\begin{aligned}\dot{V} = {} & \dot{x}_o^T\tilde{h}_o - \dot{x}_o^T\mathcal{D}\dot{x}_o - \dot{x}_o^T h_o^K(x_o) \\ & + \sum_{i=1}^N\{(\dot{p}_o^T + [\omega_o \times r_i]^T)f_i^K + \omega_o^T t_i^K\}. \end{aligned} \tag{49}$$

Employing (33) for $h_o^K(x_o)$ and rewriting the sum in terms of a dot product with $\dot{x}_o$ cancels out the last two terms in (49) and eventually yields

$$\dot{V} = \dot{x}_o^T\tilde{h}_o - \dot{x}_o^T\mathcal{D}\dot{x}_o < \dot{x}_o^T\tilde{h}_o \tag{50}$$

and thus $\rho(y) = \mathcal{D}y$ in (44). □

This result is a direct consequence of the passivity property of the subsystems, i.e. the rigid body dynamics and the closed-loop manipulator dynamics and is readily expressed in terms of end-effector wrenches/velocities.

Corollary 2. *The coupled system of object and manipulators (30), composed of the manipulator and object dynamics (1) and (8), is strictly output passive with respect to the input/output combination $u = \tilde{h}_i$ and $y = \dot{x}_i$ for any $i \in \{1, \ldots, N\}$.*

Proof. Choosing $u = \tilde{h}_i$ and $y = \dot{x}_i$ as input/output signals is equivalent to a change of the coordinate system preserving the passivity property presented in Lemma 1. By employing (10) and $\omega_o = \omega_i$ for computing $\dot{x}_i$ and transforming the wrench $\tilde{h}_o$ to an equivalent wrench $\tilde{h}_i$ one has

$$\dot{x}_i = \begin{bmatrix} I_3 & S^T(r_i) \\ 0_3 & I_3 \end{bmatrix}\dot{x}_o \quad \text{and} \quad \tilde{h}_i = \begin{bmatrix} I_3 & 0_3 \\ S^T(r_i) & I_3 \end{bmatrix}\tilde{h}_o. \tag{51}$$

It is now straightforward to verify that $\dot{x}_o^T\tilde{h}_o = \dot{x}_i^T\tilde{h}_i$ from which follows $\dot{V} < \dot{x}_i^T\tilde{h}_i$. □

Based on this passivity characterization, one readily derives stability of the cooperative manipulator system.

Theorem 3. *The cooperative manipulator system (30) is asymptotically stable about $x_o = x_o^d = const.$ for $\tilde{h}_o = 0_{6\times 1}$ in (8) and $\tilde{h}_i = 0_{6\times 1}$ in (1). Moreover, when interacting with a passive environment, i.e. the relation between $\dot{x}_o$ and $\tilde{h}_o$ is described by a strictly passive map [36, Def. 6.3], the cooperative manipulator system remains stable.*

Proof. As stated in Lemma 1, the system of object and manipulators (30) is strictly output passive. The feedback interconnection of the cooperative dynamics and the passive environment is strictly passive with input $\tilde{h}_o$ and output $\dot{x}_o$. In order to conclude on stability, we need to show that the system (30) is zero-state detectable. Here we will show that the system is zero-state observable which implies that it is also zero-state detectable. Consider the output $y = \dot{x}_o = 0_{6\times 1}$. It follows immediately that $\ddot{x}_o = 0_{6\times 1}$. Employing this and $\tilde{h}_o = 0_{6\times 1}$ in (30) one has $h_o^K(x_o, x_o^d) = 0_{6\times 1}$, which can only hold true if $\Delta p_o \equiv \Delta\epsilon_o \equiv 0_{3\times 1}$ in (33). Hence the system (30) is zero-state observable for the error state $\Delta x = (\Delta p_o^T, \Delta\varepsilon_o^T)^T$. Asymptotic stability of the cooperative manipulator system without disturbances follows immediately from application of Lemma 6.7. Stability of the manipulators in contact with a strictly passive environment follows by Theorem 6.3 in [36]. □

For the relevant case when the system is subject to non-ideal feedback linearization and externally applied wrenches we present the following result.

Theorem 4. *Assume that the external disturbance on the object $\tilde{h}_o$ in (8) and the disturbance due to non-ideal feedback linearization of the manipulators $\tilde{h}_i$ in (1) are uniformly bounded. Then x_o in (30) is uniformly ultimately bounded about $x_o^d = const.$*

Proof. The net wrench about the object's center of mass $\tilde{h}_o^\Sigma$ due to the disturbances $\tilde{h}_o$ and $\tilde{h} = [\tilde{h}_1^T, \ldots, \tilde{h}_N^T]^T$ is given by $\tilde{h}_o^\Sigma = G\tilde{h} + \tilde{h}_o$. Since the $\tilde{h}_i$'s and $\tilde{h}_o$ are bounded, $\tilde{h}_o^\Sigma$ is bounded, too. Linearization of the interaction dynamics (30) about an arbitrary equilibrium pose $\bar{x}_o$ yields

$$\mathcal{M}\delta\ddot{x}_o + \mathcal{D}\delta\dot{x}_o + \mathcal{K}\delta x_o = \tilde{h}_o^\Sigma. \tag{52}$$

It is obvious that $\mathcal{M}$ and $\mathcal{D}$ are symmetric and positive definite while $\mathcal{K}$ is in general *asymmetric*. $\mathcal{K}$ is positive definite, too, since all eigenvalues of the summand matrices in (34) are the eigenvalues of the block matrices (k_i and $\kappa_i + \|r_i\|^2 k_i$ respectively) on the diagonal. As discussed in [35, Theorem 2], the stiffness matrix $\mathcal{K}$ can always be brought into symmetric form by an appropriate change of coordinates. In fact the linearized system (52) can be diagonalized by means of a real congruence transformation if and only if $\mathcal{M}^{-1}\mathcal{D}$ commutes with $\mathcal{M}^{-1}\mathcal{K}$ [38]. Explicit computation reveals $\mathcal{D}\mathcal{M}^{-1}\mathcal{K} = \mathcal{K}\mathcal{M}^{-1}\mathcal{D}$. Thus there exists a transformation which decouples the dynamics (52) into six independent second order ODEs. Since $\mathcal{M}$, $\mathcal{D}$ and $\mathcal{K}$ are positive definite, the diagonal elements (corresponding to the eigenvalues of the matrices) are all positive, yielding (exponential) stability of the

linearized system. Furthermore, under mild assumptions [39, (8.70) through (8.74)] it can be shown that the joint space disturbances arising from non-ideal feedback linearization are bounded which leads to bounded disturbances $\tilde{h}_i$ in task space by employing the generalized inverse of the Jacobian [25] for the mapping between joint and task space. Boundedness of $\tilde{h}_o$ and $\tilde{h}_i$ and exponential stability of the linearized dynamics (52) yields (local) stability of the interaction dynamics (30) by applying Lemma 9.2 in [36]. □

This result is of prior relevance for the practical implementation of cooperative manipulation tasks. It proofs robustness of the interaction dynamics to small (bounded) perturbations arising e.g. from imperfect feedback linearization or contact with the environment. Implicitly, the robustness property has been used for the successful implementation of cooperative manipulation schemes in the past but no explicit and formal verification was presented so far incorporating the Dirac structure in the interaction model.

D. Cooperative manipulator model and control design

In this section we discuss the presented cooperative manipulator model in view of control design methodologies. To this end, consider the block scheme representation of the cooperating manipulators illustrated in Fig. 3.

The block scheme is divided into two main parts: One block corresponding to the plant model (interaction dynamics) and one block containing the controller (object-level controller) following standard control loop nomenclature. Note that the apparent end-effector dynamics result themselves from a local, individually implemented control loop as in (1) or alternatively (20). However, for the characterization of the interaction effects in cooperative manipulation tasks the apparent end-effector behavior is an essential part of the plant dynamics and thus incorporated into the interaction dynamics block. The object-level controller is exclusively in charge of implementing the desired apparent behavior (trajectory tracking, virtual impedance) of the object. To this end, suitable setpoints for the manipulators in terms of $\ddot{x}_i^d$ and h_i^d are generated. Speaking in control terms, these are the manipulated variables. The command variable is the desired object motion $\ddot{x}_o^d$ whereas the control variable is the actual object motion $\ddot{x}_o$.

In the block scheme representation in Fig. 3 it becomes obvious that the depicted object-level controller is in fact a feed forward controller. More advanced control methodologies for cooperative manipulators as e.g. [17]–[21] apply directly to our interaction dynamics model and are closing explicitly the object-level feedback loop. In particular, feeding back the h_i to the object-level controller is usually done for implementing internal/external force control schemes. However, in previous works no explicit plant model in terms of the interaction dynamics is used and as a consequence the interaction wrenches could only be assumed to be *measured* by force/torque sensors. By means of (17) and (18) we provide an explicit expression for *computing* the interaction wrench resulting in a complete and physically consistent model for the design and analysis of cooperative manipulation tasks.

E. Internal/external wrench analysis

In this section we extend and apply our recent results on the physically consistent decomposition of manipulator wrenches into external (motion-inducing) and internal (constraint-violating) wrenches. To this end, consider again the analytic expression for the interaction wrenches h in (18) and note that $h = [h_o^T, h_1^T, \ldots, h_N^T]^T$ is composed of the wrench acting on the object *and* the end-effector wrenches. In other words, the interaction wrenches h are equal to the constraining wrenches for the constrained dynamical system built by N manipulators *and* object. In general, the end-effector interaction wrenches $h' = [h_1^T, \ldots, h_N^T]^T$ contain internal and external wrench components. Since we are now interested in analyzing whether internal wrenches is applied to the manipulated object or not, we consider the reduced constrained multi-body system composed exclusively of the N manipulators and the reduced set of kinematic constraints $A'\ddot{x}' = b'$ with $A' \in \mathbb{R}^{6(N-1) \times 6N}$ and $b' \in \mathbb{R}^{6N}$. This reformulation eliminates the additional degrees of freedom inherent to the object but maintains the relative kinematic constraints between the manipulators. Based on this reduced system formulation, the internal wrenches are computed analog to (18) as the constraining wrench for the reduced system

$$h'_{\text{int}} := h'_c = M'^{\frac{1}{2}}(A'M'^{-\frac{1}{2}})^{\dagger}(b' - A'\ddot{x}'^x) \qquad (53)$$

with $M' = \text{diag}(M_1, \ldots, M_N)$ denoting the mass matrix of the reduced system and the commanded acceleration vector $\ddot{x}'^x$ obtained by inverting $h'^x = M'\ddot{x}'^x$. Note that $h'^x = [(h_1^x)^T, \ldots, (h_N^x)^T]$ is the virtual wrench resulting exclusively from the manipulators' motion controllers as defined in (6) and no internal wrench is applied whenever the commanded manipulator acceleration is compatible to the kinematic constraints. The external wrench components result now from

$$h'_{\text{ext}} = h' - h'_{\text{int}}. \qquad (54)$$

This formulation reveals the relevance of our previous results in [23] for the internal wrench analysis in cooperative manipulation tasks and puts them into the context of internal/external wrench computation. The consideration of the constraining wrenches h'_c in (53) constitutes a novel paradigm for the characterization of internal wrenches. Consequently, a consistent analysis of internal wrenches can not be performed based on the measured end-effector wrenches h' but needs to incorporate the kinematics of the end effectors as visible from (53). Descriptively speaking this means for the applied internal wrenches that it does not matter how much of the payload each manipulator carries individually as long as the commanded motion of the manipulator ensemble $\ddot{x}'^{\Sigma}$ describes a rigid body motion compatible to the imposed constraints.

V. EXPERIMENTAL EVALUATION

The conducted experimental study focuses on the evaluation of the apparent dynamics of the cooperative manipulator system presented in Theorem 2. To this end, we measure the wrench
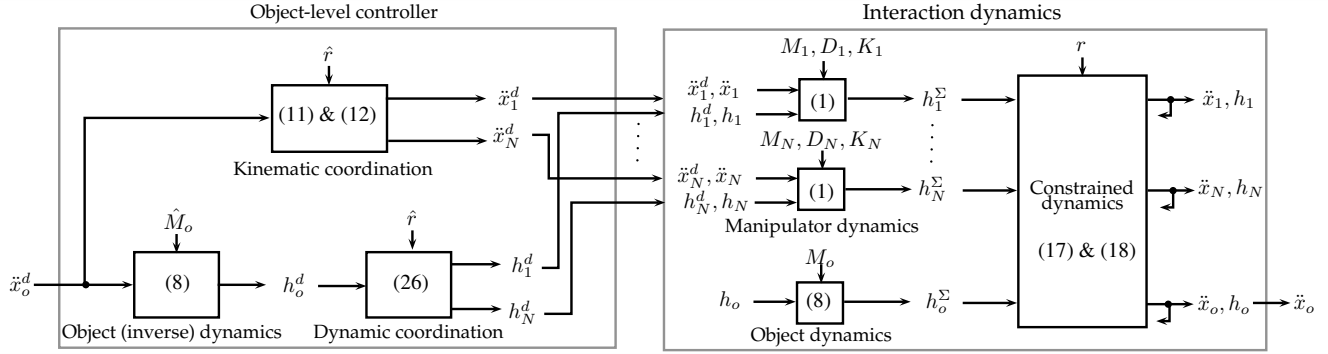
Fig. 3. Block scheme representation of the interaction dynamics model and object-level controller

$\tilde{h}_o$ and the object pose x_o in a cooperative manipulator setup and perform subsequently a system identification to estimate the parameters $\mathcal{M}$, $\mathcal{D}$ and $\mathcal{K}$.

A. Experimental setup

The experimental setup involving two anthropomorphic manipulators with 7 degrees of freedom and wrist-mounted force/torque sensors is depicted in Fig. 4.
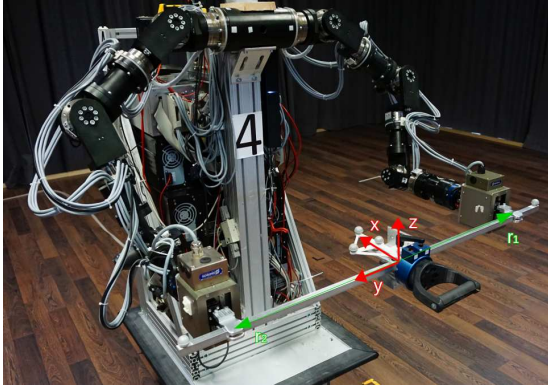

Fig. 4. Experimental setup with two robotic manipulators and force/torque sensor for measuring the externally applied wrench $\tilde{h}_o$

Both end-effectors are rigidly grasping an aluminum beam with a quadratic profile and 1.5mm edge length. The overall length of the beam is 1m. A JR3 67M25 6-dimensional force/torque sensor is attached to the center of the beam and an auxiliary handle is mounted on the opposite site of the sensor, enabling the measurement of the externally applied wrench $\tilde{h}_o$. The force/torque signal is filtered by a low-pass filter with 500Hz cutoff frequency. Simultaneously, the object is equipped with optical markers in order to track its pose x_o via a Qualisys Motion Capture System. The object coordinate frame $\{o\}$ coincides with the center of mass and is indicated by means of red arrows in Fig. 4. The overall mass of the object is $m_o = 1.75$kg and its moment of inertia about the x-axis is $J_{o,x} \approx 0.055$kgm^2.

The manipulators are controlled individually by an impedance control scheme according to (1) with a sampling time of $T_s = 1$ms, wherein the desired wrench is set to zero, i.e. $h_i^d = 0_{6\times 1}$ and a constant desired end-effector pose,

i.e. x_i^d = const., such that $r_1 = (0.0, -0.40, 0.0)^T$m and $r_2 = (0.0, +0.40, 0.0)^T$m. The impedance control parameters for both manipulators are $m_i = 10$kg, $d_i = 180\frac{\text{Ns}}{\text{m}}$, $k_i = 300\frac{\text{N}}{\text{m}}$ for the translational behavior and $J_i = I_3 \cdot 0.5$kgm^2, $\delta_i = 10$Nm$\frac{\text{rad}}{\text{s}}$, $\kappa_i = 50\frac{\text{Nm}}{\text{rad}}$ for the rotational behavior.

B. Translational dynamics

The apparent translational dynamics in x-direction derived from (30) can be written as

$$m_o^* \ \ddot{p}_x + d_o^* \ \dot{p}_x + k_o^* \ p_x = \tilde{f}_x \tag{55}$$

with the object's position in x-direction $p_x \in \mathbb{R}$, the applied force in x-direction $\tilde{f}_x \in \mathbb{R}$ and the translational impedance parameters

$$m_o^* = 21.75\text{kg}, \quad d_o^* = 360\frac{\text{Ns}}{\text{m}}, \quad k_o^* = 600\frac{\text{N}}{\text{m}} \tag{56}$$

extracted from the matrices $\mathcal{M}$, $\mathcal{D}$ and $\mathcal{K}$ in Theorem 2. The applied force $\tilde{f}_x$ and the position p_x are plotted in Fig. 5.
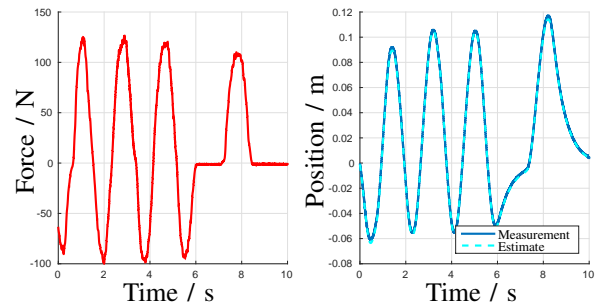

Fig. 5. Externally applied force and resulting position in x-direction

Based on the reduced dynamical model (55) and the input/output data given by $\tilde{f}_x/p_x$, a system identification is performed. Estimates of the scalar parameters m_o^*, d_o^* and k_o^* are obtained using the linear grey-box model estimation method (greyest) of the Matlab System Identifcation Toolbox. The estimates are

$$\hat{m}_o^* = 21.5\text{kg}, \quad \hat{d}_o^* = 384\frac{\text{Ns}}{\text{m}}, \quad \hat{k}_o^* = 630\frac{\text{N}}{\text{m}}. \tag{57}$$

The identified model parameters correspond very well to their nominal values as indicated in (56). The model output for the

input depicted on the left-hand side of Fig. 5 and the estimated parameters (57) is illustrated by the dashed line on the right-hand side of Fig. 5, yielding a mean squared error $\|\hat{p}_x - p_x\|^2$ of $3.86 \cdot 10^{-6} \text{m}^2$ for a recording interval of 45s. Estimated and measured values coincide well and prove consistency of the presented approach.

C. Rotational dynamics

The apparent rotational dynamics about the object's z-axis derived from (30) can be written as

$$J^*_{o,z} \ddot{\varphi}_z + d^*_o \dot{\varphi}_z + k^*_o \varphi_z = \tilde{t}_z \tag{58}$$

with the object's orientation about the x-axis $\varphi_x \in \mathbb{R}$, the applied torque about the x-axis $\tilde{t}_x \in \mathbb{R}$ and the rotational impedance parameters

$$J^*_{o,z} = 4.255 \text{kgm}^2, \quad \delta^*_{o,z} = 77.6 \text{Nm}\frac{\text{rad}}{\text{s}}, \quad \kappa^*_{o,z} = 196\frac{\text{Nm}}{\text{rad}}. \tag{59}$$

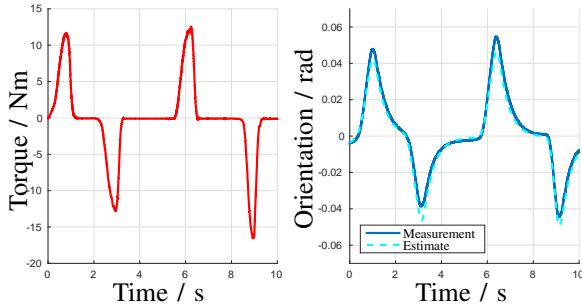The applied torque $\tilde{t}_z$ and the resulting orientation φ_z are plotted in Fig. 6.

Fig. 6. Externally applied torque and resulting orientation about the z-axis

The estimates for the rotational dynamics in (58) are

$$\hat{J}^*_{o,z} = 4.652 \text{kgm}^2, \quad \hat{\delta}^*_{o,z} = 84 \text{Nm}\frac{\text{rad}}{\text{s}}, \quad \hat{\kappa}^*_{o,z} = 170\frac{\text{Nm}}{\text{rad}}. \tag{60}$$

The identified rotational impedance parameters approximate their nominal values well. The most significant divergence is observed for the rotational stiffness. The identified value $\hat{\kappa}^*_{o,z}$ is slightly smaller than predicted. This result is attributed to a finite stiffness of the mechanical arrangement whereas an ideal rigid structure is assumed for computing $\kappa^*_{o,z}$. The model output for the estimated parameters is illustrated by the dashed line on the right-hand side of Fig. 6, yielding a mean squared error $\|\hat{\varphi}_x - \varphi_x\|^2$ of $2.46 \cdot 10^{-5} \text{rad}^2$ for a recording interval of 60s.

D. Dynamics in SE(3)

For the identification of the impedance parameters in $SE(3)$ the (linearized) dynamics of the cooperating manipulators are used as presented in (52). For the manipulator setup under consideration the object impedance parameters are

$$\mathcal{M}^* = [21.75 \text{kg} \cdot I_3, 0_3; 0_3, \text{diag}([4.255, 1, 4.255]) \text{kgm}^2]$$
$$\mathcal{D}^* = [360\frac{\text{Ns}}{\text{m}}, 0_3; 0_3, \text{diag}([78, 20, 78]) \text{Nm}\frac{\text{rad}}{\text{s}}] \tag{61}$$
$$\mathcal{K}^* = [600\frac{\text{N}}{\text{m}}, 0_3; 0_3, \text{diag}([196, 100, 196]) \frac{\text{Nm}}{\text{rad}}].$$

The wrench $\tilde{h}_o$ applied to the object and the resulting object pose δx_o are plotted in Fig. 7.
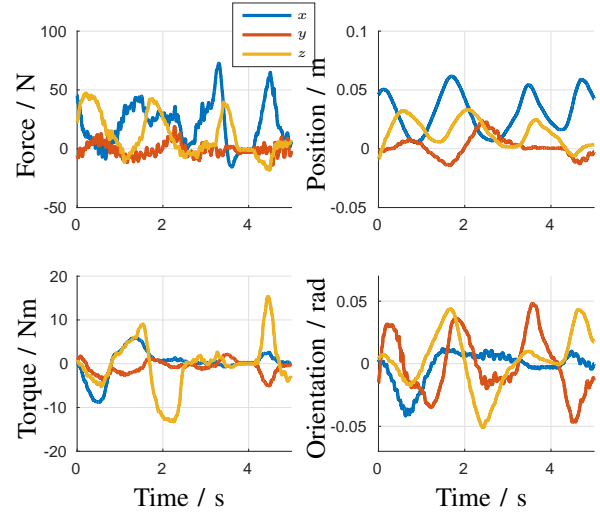

Fig. 7. Applied object wrench $\tilde{h}_o$ and resulting object pose δx_o in $SE(3)$

The estimates of the object impedance parameters in (52) for a recording interval of 30s are

$$\hat{\mathcal{M}}^* = [25.8 \text{kg} \cdot I_3, 0_3; 0_3, \text{diag}([2.8, 0.45, 2.8]) \text{kgm}^2]$$
$$\hat{\mathcal{D}}^* = [485\frac{\text{Ns}}{\text{m}}, 0_3; 0_3, \text{diag}([73, 19, 73]) \text{Nm}\frac{\text{rad}}{\text{s}}] \tag{62}$$
$$\hat{\mathcal{K}}^* = [820\frac{\text{N}}{\text{m}}, 0_3; 0_3, \text{diag}([148, 78, 148]) \frac{\text{Nm}}{\text{rad}}].$$

The estimated values provide a satisfactory approximation of the nominal impedance parameters. The most significant divergence is observed for the estimates of the rotational inertia, yielding too small values. This observation is explained through a comparatively low excitation of the rotational motion in combination with the finite structural stiffness of the object. However, the rotational damping is perfectly identified. The translational parameters match satisfactory. Moreover, the experimental study shows clearly the relevance of the coupling between the translational and rotational impedance parameters for the apparent object impedance.

VI. CONCLUSIONS

In this article we present a novel approach to the modeling of the interaction dynamics in cooperative manipulation tasks. Our approach incorporates explicitly the kinematic constraints imposed by the cooperatively manipulated object in task space and provides for the first time a closed-form expression for the emerging interaction wrenches. The proposed model is physically consistent and suitable for the analysis of dynamic cooperative manipulation tasks. By deriving fundamental system

properties such as passivity and stability, we demonstrate that the cooperative manipulator system exhibits desirable properties which haven been exploited implicitly for the control design. The presented model is a mandatory prerequisite for a systematic model-based control design. Moreover, we present a new paradigm for the decomposition of the manipulator wrenches into internal and external components and derive the apparent object dynamics when interacting with the environment. An experimental study by means of two cooperating anthropomorphic manipulators confirms the significance of the presented results for cooperative manipulation tasks.

ACKNOWLEDGMENT

REFERENCES

[1] S. Hayati, "Hybrid position/force control of multi-arm cooperating robots," in *Robotics and Automation. Proceedings. 1986 IEEE International Conference on*, vol. 3, pp. 82–89, Apr 1986.

[2] O. Khatib, "Object manipulation in a multi-effector robot system," in *Proceedings of the 4th International Symposium on Robotics Research*, (Cambridge, MA, USA), pp. 137–144, MIT Press, 1988.

[3] M. Unseren and A. Koivo, "Reduced order model and decoupled control architecture for two manipulators holding an object," in *Robotics and Automation, 1989. Proceedings., 1989 IEEE International Conference on*, pp. 1240–1245 vol.2, May 1989.

[4] M. D. Djurovic and M. K. Vukobratovic, "A contribution to dynamic modeling of cooperative manipulation," *Mechanism and Machine Theory*, vol. 25, no. 4, pp. 407 – 415, 1990.

[5] X. Yun and V. R. Kumar, "An approach to simultaneous control of trajectory and interaction forces in dual-arm congurations," *IEEE Transactions on Robotics and Automation*, pp. 618–624, 1991.

[6] J. Gudio-Lau and M. A. Arteaga, "Dynamic model and simulation of cooperative robots: a case study," *Robotica*, vol. 23, pp. 615–624, 9 2005.

[7] H. Bruyninckx and O. Khatib, "Gauss' Principle and the Dynamics of Redundant and Constrained Manipulators," in *International Conference on Robotics and Automation*, vol. 3, pp. 2563–2568, 2000.

[8] V. De Sapio and O. Khatib, "Operational space control of multibody systems with explicit holonomic constraints," in *Robotics and Automation, 2005. ICRA 2005. Proceedings of the 2005 IEEE International Conference on*, pp. 2950–2956, April 2005.

[9] S. Stramigioli, *Modeling and IPC Control of Interactive Mechanical Systems: A Coordinate-Free Approach*. Secaucus, NJ, USA: Springer-Verlag New York, Inc., 2001.

[10] T. J. Courant, "Dirac manifolds," *Transactions of the American Mathematical Society*, vol. 319, no. 2, pp. 631–661, 1990.

[11] H. Yoshimura and J. E. Marsden, "Representations of dirac structures and implicit port-controlled lagrangian systems," in *18th International Symposium on Mathematical Theory of Networks and Systems*, 2008.

[12] A. van der Schaft, "Port-hamiltonian systems: an introductory survey," in *Proceedings of the International Congress of Mathematicians Vol. III: Invited Lectures* (M. Sanz-Sole, J. Soria, J. Varona, and J. Verdera, eds.), (Madrid, Spain), pp. 1339–1365, European Mathematical Society Publishing House (EMS Ph), 2006.

[13] A. Bicchi, D. Prattichizzo, and C. Melchiorri, "Force and dynamic manipulability for cooperating robot systems," in *in Proc. Int. Symp. on Robotic Systems (IROS97*, pp. 1479–1484, 1997.

[14] S. Arimoto, K. Tahara, J.-H. Bae, and M. Yoshida, "A stability theory of a manifold: concurrent realization of grasp and orientation control of an object by a pair of robot fingers," *Robotica*, vol. 21, no. 02, pp. 163–178, 2003.

[15] J. Fink, N. Michael, S. Kim, and V. Kumar, "Planning and control for cooperative manipulation and transportation with aerial robots," *The International Journal of Robotics Research*, vol. 30, no. 3, pp. 324–334, 2011.

[16] N. Hogan, "Impedance control: An approach to manipulation," in *American Control Conference, 1984*, pp. 304–313, June 1984.

[17] S. Schneider and J. Cannon, R.H., "Object impedance control for cooperative manipulation: theory and experimental results," *Robotics and Automation, IEEE Transactions on*, vol. 8, pp. 383–394, Jun 1992.

[18] K. Kosuge, H. Yoshida, T. Fukuda, M. Sakai, K. Kanitani, and K. Hariki, "Unified control for dynamic cooperative manipulation," in *Intelligent Robots and Systems. Proceedings of the IEEE/RSJ/GI International Conference on*, vol. 2, pp. 1042–1047 vol.2, Sep 1994.

[19] J. Szewczyk, G. Morel, and P. Bidaud, "Distributed impedance control of multiple robot systems," in *Robotics and Automation, 1997. Proceedings., 1997 IEEE International Conference on*, vol. 2, pp. 1801–1806 vol.2, Apr 1997.

[20] F. Caccavale, V. Lippiello, G. Muscio, F. Pierri, F. Ruggiero, and L. Villani, "Grasp planning and parallel control of a redundant dual-arm/hand manipulation system," *Robotica*, vol. 31, pp. 1169–1194, 10 2013.

[21] T. Wimböck, C. Ott, A. Albu-Schäffer, and G. Hirzinger, "Comparison of object-level grasp controllers for dynamic dexterous manipulation," *The International Journal of Robotics Research*, vol. 31, no. 1, pp. 3–23, 2012.

[22] A. Macchelli, "Passivity-based control of implicit port-hamiltonian systems," in *Control Conference (ECC), 2013 European*, pp. 2098–2103, July 2013.

[23] S. Erhart and S. Hirche, "Internal force analysis and load distribution for cooperative multi-robot manipulation," *IEEE Transactions on Robotics (T-RO)*, vol. 31, no. 5, pp. 1238 – 1243, 2015.

[24] C. F. Gauß, "Über ein neues allgemeines Grundgesetz der Mechanik.," *Journal für die reine und angewandte Mathematik*, vol. 4, pp. 232–235, 1829.

[25] O. Khatib, "A unified approach for motion and force control of robot manipulators: The operational space formulation," *Robotics and Automation, IEEE Journal of*, vol. 3, pp. 43–53, February 1987.

[26] C. Ott, A. Albu-Schäffer, A. Kugi, S. Stamigioli, and G. Hirzinger, "A passivity based cartesian impedance controller for flexible joint robots - part i: torque feedback and gravity compensation," in *Robotics and Automation, 2004. Proceedings. ICRA '04. 2004 IEEE International Conference on*, vol. 3, pp. 2659–2665 Vol.3, April 2004.

[27] J. Diebel, "Representing attitude: Euler angles, unit quaternions, and rotation vectors," tech. rep., Stanford Univ., CA, United States, 2006.

[28] F. Caccavale, P. Chiacchio, A. Marino, and L. Villani, "Six-dof impedance control of dual-arm cooperative manipulators," *Mechatronics, IEEE/ASME Transactions on*, vol. 13, no. 5, pp. 576–586, 2008.

[29] F. E. Udwadia and R. E. Kalaba, "A new perspective on constrained motion," *Proceedings: Mathematical and Physical Sciences*, vol. 439, no. 1906, pp. 407–410, 1992.

[30] P. Chiachio, S. Chiaverini, L. Sciavicco, and B. Siciliano, "Task space dynamic analysis of multiarm system configurations," *Int. J. Rob. Res.*, vol. 10, pp. 708–715, Dec. 1991.

[31] R. Volpe and P. Khosla, "A theoretical and experimental investigation of explicit force control strategies for manipulators," *IEEE Transactions on Automatic Control*, vol. 38, pp. 1634–1650, 1993.

[32] O. Khatib, K. Yokoi, K. Chang, D. Ruspini, R. Holmberg, A. Casal, and A. Baader, "Force strategies for cooperative tasks in multiple mobile manipulation systems," in *Robotics Research*, pp. 333–342, 1996.

[33] M. Uchiyama and P. Dauchez, "A symmetric hybrid position/force control scheme for the coordination of two robots," in *Robotics and Automation, 1988. Proceedings., 1988 IEEE International Conference on*, pp. 350–356 vol.1, Apr 1988.

[34] H.-C. Lin, T.-C. Lin, and K. Yae, "On the skew-symmetric property of the newton-euler formulation for open-chain robot manipulators," in *American Control Conference, Proceedings of the 1995*, vol. 3, pp. 2322–2326 vol.3, Jun 1995.

[35] J. Loncaric, "Normal forms of stiffness and compliance matrices," *Robotics and Automation, IEEE Journal of*, vol. 3, pp. 567–572, December 1987.

[36] H. Khalil, *Nonlinear Systems*. Prentice Hall, 2002.

[37] R. Ortega and M. Spong, "Adaptive motion control of rigid robots: a tutorial," in *Decision and Control, 1988., Proceedings of the 27th IEEE Conference on*, pp. 1575–1584 vol.2, Dec 1988.

[38] T. Caughey and M. Okelly, "Classical normal modes in damped linear dynamic systems," *Journal of Applied Mechanics*, vol. 32, no. 3, pp. 583–588, 1965.

[39] B. Siciliano, L. Sciavicco, L. Villani, and G. Oriolo, *Robotics: Modelling, Planning and Control*. Springer Publishing Company, Incorporated, 1st ed., 2008.